HHS Public Access

Author manuscript

Curr Biol. Author manuscript; available in PMC 2015 June 08.

Published in final edited form as:

Curr Biol. 2013 December 16; 23(24): 2481–2490. doi:10.1016/j.cub.2013.10.053.

Combinatorial Rules of Precursor Specification Underlying Olfactory Neuron Diversity

Qingyun Li[1], **Tal Soo Ha**[4,6], **Sumie Okuwa**[1], **Yiping Wang**[1], **Qian Wang**[3], **S. Sean Millard**[5], **Dean P. Smith**[4], and **Pelin Cayirlioglu Volkan**[1,2,*]

[1]Department of Biology, Duke University, Durham, NC 27708, USA

[2]Duke Institute for Brain Sciences, Durham, NC 27708, USA

[3]The Pratt School of Engineering, Duke University, Durham, NC 27708, USA

[4]Department of Pharmacology and Center for Basic Neuroscience, University of Texas Southwestern Medical Center, Dallas, TX 75390, USA

[5]School of Biomedical Sciences, The University of Queensland, Brisbane, QLD 4072, Australia

Summary

Background—Sensory neuron diversity ensures optimal detection of the external world and is a hallmark of sensory systems. An extreme example is the olfactory system, as individual olfactory receptor neurons (ORNs) adopt unique sensory identities by typically expressing a single receptor gene from a large genomic repertoire. In *Drosophila,* about 50 different ORN classes are generated from a field of precursor cells, giving rise to spatially restricted and distinct clusters of ORNs on the olfactory appendages. Developmental strategies spawning ORN diversity from an initially homogeneous population of precursors are largely unknown.

Results—Here we unravel the nested and binary logic of the combinatorial code that patterns the decision landscape of precursor states underlying ORN diversity in the *Drosophila* olfactory system. The transcription factor Rotund (Rn) is a critical component of this code that is expressed in a subset of ORN precursors. Addition of Rn to preexisting transcription factors that assign zonal identities to precursors on the antenna subdivides each zone and almost exponentially increases ORN diversity by branching off novel precursor fates from default ones within each zone. In *rn* mutants, *rn*-positive ORN classes are converted to *rn*-negative ones in a zone-specific manner.

Conclusions—We provide a model describing how nested and binary changes in combinations of transcription factors could coordinate and pattern a large number of distinct precursor identities within a population to modulate the level of ORN diversity during development and evolution.

*Correspondence: pc72@duke.edu.

[6]Present address: Department of Biomedical Science, College of Natural Science, Daegu University, 15 Naeri, Jillyang, Gyeongsan, Gyeongbuk 712-714, South Korea

Supplemental Information

Supplemental Information includes seven figures and Supplemental Experimental Procedures and can be found with this article online at http://dx.doi.org/10.1016/j.cub.2013.10.053.

Introduction

Faithful detection of a vast variety of sensory cues in the environment is essential for animal survival and reproduction. To increase the detection coverage of a complex sensory environment, animals have evolved large numbers of specialized classes of neurons, each with a distinct sensitivity spectrum that depends on the identity of the sensory receptors that they express. A remarkable example of this cellular diversity is seen in vertebrate and insect olfactory systems, where extreme sensory and functional specialization of individual olfactory receptor neurons (ORNs) is accompanied by a high level of diversity of ORN classes at the systems level. Singular expression of olfactory receptor genes from a large gene family pool defines individual ORN classes and serves as the molecular underpinning of ORN diversity. Developmental mechanisms spawning this extraordinary diversity of ORN classes from an initially homogenous population of precursors remain unknown.

Due to the stereotypical spatial organization of fly ORN classes into distinct “sensilla” zones on the surface of olfactory appendages, the adult *Drosophila* olfactory system is a great model to approach the problem of ORN diversification. In flies, approximately 50 different ORN classes are organized in clusters of one to four neurons within sensilla on antennae and maxillary palps [1]. Antennal sensilla have three major morphological types that occupy distinct zones: basiconic, trichoid, and coeloconic [1]. Basiconic sensilla have further morphological and zonal subdivisions into small, large, and thin basiconics [2] (Figure 1A). ORNs in basiconic and trichoid sensilla typically express seven-transmembrane odorant receptors (ORs), whereas ionotropic receptors (IRs) are expressed by the coeloconic ORNs [1–5]. Each morphologically distinct sensilla zone is further segmented into generally four, sometimes three subzones based on sensilla subtypes, each of which houses a unique set of ORNs that express an invariable combination of olfactory receptors (Figure 1B) [2]. All ORNs expressing the same receptor in a certain zone target their axons to a single synaptic structure, called a glomerulus, in the antennal lobe where they relay information to second-order neurons.

ORNs in each sensillum are siblings derived from asymmetric divisions of distinct sensory organ precursors (SOPs) [1]. We reason that SOP differentiation potentials determine spatially segregated sensilla type and subtype identities, represented by the allowable set of receptors to be expressed in a given lineage. Therefore, patterning and diversification of SOP identities for each sensillum is the initial step in ORN diversification. It is implied that combinatorial expression of multiple transcription factors—Amos, Atonal (Ato), and Lozenge (Lz)—dictates sensilla type lineages [6–9]. However, the molecular mechanism for sensilla subtype diversification within each sensilla type zone, a key regulatory step in ORN specification, is unknown.

Here we show that a Krüppel-like transcription factor, Rotund (Rn), cell autonomously fine tunes the differentiation potential of SOPs, thereby regulating sensilla subtype specification by branching off novel precursor fates from default ones in each zone. Rn is expressed in a subset of ORN precursors, which give rise to 18 ORN classes clustered within eight different antennal sensilla subtypes. Within each sensilla type, subtypes are identified as either *rn* positive or *rn* negative. A comprehensive analysis of *rn* mutants demonstrates that

ORNs in *rn*-positive sensilla subtypes are converted to specific *rn*-negative ones within each zone. Olfactory receptors expressed in *rn*-positive ORNs (but not *rn*-negative ones) require a common regulatory motif M1 for expression, as the replacement of this motif abolishes the antennal expression of *rn*-positive receptors. In conjunction with the phenotypic analysis of previously identified factors that have early functions in ORN specification, we demonstrate a nested combinatorial strategy by which transcription factors are assembled together to progressively impose hierarchical and lineage-specific restrictions on ORN precursor differentiation potentials in order to generate ORN diversity. This nested organizational logic among a limited number of transcription factors provides an extremely efficient solution that potentially could be utilized in many other neural differentiation processes when high population diversity benefits survival. Based on this logic, we model the decision landscape for precursor cell fates that coordinately unfolds the segmented distribution of ~40 adult ORN classes within the antennal olfactory appendage. Our model shows that elimination or addition of new gene regulatory modules to preexisting combinations can lead to binary precursor cell-fate changes and dramatically influence the level of ORN diversity in the olfactory system.

Results

Rn Is Expressed in a Subset of Antennal ORN Precursors

To understand the regulation of olfactory receptor expression and ORN diversification, we analyzed two previously isolated mutants, $tod^{Z3\text{-}6129}$ and $tot^{Z3\text{-}4626}$ [10]. In both alleles, the antennal odorant receptor Or67d, expressed by ORNs singly housed in the trichoid subtype at1 sensilla, is absent, and the DA1 glomerulus targeted by these receptor neurons in the antennal lobe is missing (Figure 1C). Sequence information revealed that both $tod^{Z3\text{-}6129}$ and $tot^{Z3\text{-}4626}$ mutants have lesions in the *rotund* (*rn*) gene, encoding a Krüppel-like zinc-finger transcription factor with several putative splice variants, the major three of which are called E, F, and C isoforms [11] (Figure 1D). All three isoforms can be detected in the developing pupal antennae by RT-PCR. The $tod^{Z3\text{-}6129}$ allele harbors a lesion predicted to change the conserved arginine (R565) to glutamine (Q) in the shared zinc-finger domain without lowering the overall RNA levels. The $tot^{Z3\text{-}4626}$ allele contains a 37-nucleotide insertion 63 base pairs upstream of the C isoform start codon, leading to significant reductions in F and C isoform transcripts (see Figure S1A available online). We also used a previously reported hypomorphic allele, rn^{89GAL4}, in which the inserted GAL4 disrupts the gene function and recapitulates the endogenous gene expression [11]. This GAL4 line was shown to be a faithful expression reporter for *rn* in the antennal disc by RNA in situ hybridization, but not for the *roughened eye* (*roe*) gene, which is a part of the same gene locus but expresses a different transcript [11]. Transheterozygous $tod^{Z3\text{-}6129}/rn^{89GAL4}$, $tot^{Z3\text{-}4626}/rn^{89GAL4}$, and $tod^{Z3\text{-}6129}/tot^{Z3\text{-}4626}$ all produce the same phenotype as $tod^{Z3\text{-}6129}$ and $tot^{Z3\text{-}4626}$ homozygous mutants (Figure 1C; Figure S1B). Therefore, we have identified $tod^{Z3\text{-}6129}$ and $tot^{Z3\text{-}4626}$ as two new alleles of *rn*, and we will hereafter refer to them as rn^{tod} and rn^{tot}.

To understand the role of Rn in the specification of at1 ORNs, we analyzed the *rn* expression pattern in developing antennae using the enhancer-trap line rn^{89GAL4} to drive

GFP expression. In third-instar larval antennal discs, a GFP signal was detected in the central ring, representing precursors of ORNs in the olfactory segment of antennae [7] (Figure 2A; Figure S2A). At 35 hr after puparium formation (APF), *rn* expression occupies the mediolateral region of the developing antennae. At 45 hr APF, *rn* is expressed both in neurons and nonneuronal cells. *rn* expression cannot be detected in the adult olfactory appendages.

Using a FLP/FRT-mediated lineage tracing system (Supplemental Experimental Procedures), we identified 18 *rn*-positive ORN classes in the adult olfactory system clustered within eight distinct antennal sensilla subtypes (Figure 2B, left in graph and top in table; Figure S2B). Subsets of all three major types of sensilla were found to be *rn* positive. Among these subtypes, two belong to trichoid sensilla (at1 and at3), three are basiconic (thin: ab5; small: ab7, ab10), two are coeloconic (ac1 and ac4), and one is the rare intermediate type sensilla (ai1) [2, 4, 5, 12, 13]. None of the maxillary palp ORNs express *rn* (Figure S2B).

Rn Branches Off Novel ORN Precursor Fates from Default Ones in Trichoid Sensilla

Within the trichoid sensilla subtypes, *rn* is expressed in at1 and at3 lineage precursors, but not in at4 or at2 (Figure 2B, left in graph and top in table). Since at1 ORNs are abolished in *rn* mutants, we asked whether a similar effect is observed in at3 sensilla. at3 sensilla house three ORN classes that express Or2a, Or19a/b, and Or43a [2, 5]. We analyzed OR expression by at3 ORNs and found that the expression of all three OR genes and their target glomeruli were absent in *rn* mutants (Figure 3A). These results suggest that Rn regulates the specification of *rn*-positive ORNs in trichoid sensilla.

The loss of ORNs in at1 and at3 in *rn* mutants could arise either from the loss of these sensilla subtypes by cell death or from their conversion to one or more other subtypes. We tested for conversion to the at4 sensilla subtype because we found significant increases in the sizes of glomeruli innervated by *rn*-negative at4 ORNs in *rn* mutants (Figure 3B, bottom right). at4 sensilla house the cell bodies of Or47b-, Or88a-, and Or65a-expressing ORNs, which target VA1v, VA1d, and DL3 glomeruli in the antennal lobe, respectively [2, 5]. In *rn* mutants, we found that Or47b, Or88a, and Or65a expression expands to medial zones within the antenna that are normally occupied by at1 and at3 sensilla in a cell-autonomous manner (Figure 3B, top; Figures S1C, S1D, and S3A). Double labeling of Or47b and Or88a or Or65a cell bodies showed that the OR pairings in at4 were retained in the expanded antennal zones in *rn* mutants (Figure 3B, bottom left; Figure S3A). The increases in the numbers of at4 ORNs in *rn* mutants strongly suggest that *rn*-positive at1 and at3 subtypes are converted to *rn*-negative at4 sensilla. If this is true, the converted Or47b ORN population should overlap with rn^{89GAL4}-driven reporter expression in *rn* mutants. Indeed, two classes of Or47b neurons were observed in the developing antenna of *rn* mutants: Or47b ORNs that are in the endogenous at4 sensilla negative for the *rn* expression reporter, and the Or47b neurons positive for the *rn* reporter that are converted from at1 and at3 sensilla (Figure 3C). We also used the lineage-tracing method described above to analyze *rn*-positive ORN projections in *rn* mutant antennal lobes. In agreement with the conversion model, we observed the innervation of VA1v, VA1d, and DL3 glomeruli targeted by at4 ORNs, which

are normally *rn* negative in the wild-type (Figure 2B). OR expression in at2 ORNs is unaffected (Figure 3D). These results suggest that Rn diverges new trichoid ORN identities (at1 and at3) from a "default" at4 identity (Figure 3E). Overexpression of an upstream activating sequence (UAS)-*rn* transgene [11] in all trichoid and basiconic lineage precursors using *amos*-GAL4 leads to an increase of *rn*-positive at3 sensilla ORNs and a decrease in the *rn*-negative at4 ORNs (Figure S1E). However, we also detected a decrease in *rn*-positive at1 ORNs. Even though this might suggest that ectopic at3 fates can be induced by Rn overexpression, the decrease in at4 (and at1) might also arise from the toxicity of high levels of Rn, as expressing this transgene in *rn*-positive lineages in the wild-type background leads to a loss of *rn*-positive ORNs, and it is unable to rescue the OR expression phenotype in the mutant flies (Figure S1B′).

Rn Branches Off Novel ORN Precursor Fates from Default Ones in Basiconic and Coeloconic Sensilla

Next, we extended our study to nontrichoid sensilla, and we found that Rn plays a similar role in specifying ORNs in these sensilla. In both coeloconic and basiconic cases, absent *rn*-positive sensilla were converted to certain default *rn*-negative sensilla subtype identities in a lineage-specific manner, as was confirmed by the lineage-tracing experiment in *rn* mutants (Figures 2B, 4A, and 4B; Figures S3 and S4). For the coeloconic subtypes, we observed the expansion of the default ac2 sensilla into antennal zones that are normally occupied by ac1 and ac4 in *rn* mutants (Figure 4A; Figures S3C–S3F). Similar conversion effects were seen for basiconics within and among their morphological subdivisions in the absence of Rn (Figure 4B; Figure S4). Intermediate sensilla have only one *rn*-positive subtype ai1, which is lost in *rn* mutants (Figure 3B). RT-PCR was also performed on selective OR genes to confirm our genetic findings (Figure S3G). Taken together, these results suggest that Rn is responsible for the divergence of novel ORN precursor identities from default sensilla subtype precursors (Figures 3E, 4C, and 4D).

Lineage Specification by Nesting the Transcription Factor Functions Drives Precursor Cell Diversification

Since Rn expression is early and partially overlaps with the pattern of the proneural gene *amos* and the SOP marker *senseless* (*sens*) (Figure 2A; Figure S2A), we reasoned that the conversions in *rn* mutants occur due to the alterations in lineage-specific SOP identities and the corresponding combinations of olfactory receptors that have the potential to be expressed in that lineage. Indeed, the development of both endogenous and ectopic at4 ORNs in *rn* mutants is *amos* dependent, as *rn* and *amos* double mutants lack all basiconic and trichoid sensillla, including at4 (Figure 5). Futhermore, *rn* and *lozenge* (*lz*) double mutants show subtype conversion of at1 to at4 in both the endogenous trichoid zone and the duplicated ectopic zone, which is converted from basiconic to trichoid sensilla due to *lz* mutation [15] (Figure 5; Figure S5). These results support lineage-specific precursor fate conversions in *rn* mutants and reveal the bifurcating and nested nature of fate diversification among precursor cells within lineages.

A Common Motif Upstream of *rn*-Positive OR/IR Genes Is Required for Their Expression

We predicted that the transcription factor Rn regulates the olfactory receptor gene combinations allowed in a precursor lineage, either directly or indirectly, by regulating the status of the promoters of olfactory receptor genes. We used a de novo motif finding approach to search for a consensus sequence shared by the promoters of OR genes expressed in *rn*-positive, but not *rn*-negative, lineages (Supplemental Experimental Procedures). The top-scoring motif (M1) from three independent programs (MEME, PRIORITY, and WEEDER) [16–18] is [TG] GGTTGGGA [GAT] [AG] (Figure 6A). We confirmed the presence of this motif in *rn*-positive ORs/IRs and its absence in *rn*-negative ones using the known motif searching tool MAST (Figure S6A) [19]. To test whether M1 is required for *rn*-positive OR expression, we generated Or49a$^{\Delta M1}$-GAL4 and Or82a$^{\Delta M1}$-GAL4 promoter reporter lines in which M1 is replaced by a random sequence. We found significant decreases in the cells labeled by these two transgenic reporter lines, suggesting the involvement of the M1 motif in the activation of Or49a and Or82a expression (Figure 6B). We speculated that Rn may interact with this motif in a given precursor to determine the allowable receptor genes that can be expressed in ORNs from that lineage. However, we could not detect the binding of Rn to these promoters using a yeast one-hybrid (Y1H) assay, even though direct interactions with variable strengths between known DNA-binding proteins and corresponding DNA elements were seen as expected [20, 21] (Figure S6B). A recent study used electrophoretic mobility shift assay with in vitro-translated Rn to demonstrate the binding of Rn to the motif T13, which appears to be different from the M1 motif [22]. We were unable to detect the binding of Rn to T13 in our Y1H assay (Figure S6B). In addition, a sequence (856 bp upstream of the Or49a start codon) almost identical to T13 is present in the Or49a promoter, which was not bound by Rn in our Y1H assay. It is possible that yeast lacks proteins required for the proper folding and processing of Rn, or cofactors that facilitate the binding of Rn to this sequence. Further analysis of upstream regulatory sequences of OR/IR genes did not produce any correlation between the presence of T13 and the lineages of OR/IR genes (data not shown). These results suggest that Rn may not bind to OR/IR regulatory elements but perhaps regulates or interacts with other factors to determine sensilla-specific combinations of OR expression.

A Decision Landscape for Antennal ORN Precursor Diversification

How can the complex landscape of different ORN fates be carved from a homogeneous plane of precursors? The systematic analysis of the *rn* mutant phenotype in ORN diversity suggests that Rn functions to increase the diversity from each lineage but generates different ORN outcomes based on the historic and molecular contingency of the precursors. Our results along with previously identified factors expressed in subsets of precursors [6–9, 23] suggest that the final patterning of antennal olfactory receptor choice is an outcome of combinations of transcription factors functioning in a nested fashion to bifurcate and diversify precursor cells' identities (Figure 7A). These combinations encode sensilla type and subtype identities to determine olfactory receptor pairings allowed in a given precursor lineage by exerting their effects, directly or indirectly, on olfactory receptor genes. We found that Rn is a critical component of this nested control mechanism to diverge *rn*-positive sensilla subtypes from otherwise default *rn*-negative ones in each lineage-specific

precursor, leading to a dramatic increase of ORN classes in the olfactory system. Engrailed (En) and Dachshund (Dac) are two other factors with restricted and nonoverlapping expression in a proportion of sensilla subtype precursors and adult ORNs, and their mutations are associated with a lineage-specific decrease in the expression of ORs [23]. Mapping En and Dac onto the lineage decision tree based on their expression pattern showed that both genes act in a binary fashion similar to Rn to diversify specific precursor lineages (Figure 7A). However, no fate conversion event was reported in these mutants, suggesting that different functional modes may be adopted by En and Dac. Particularly, we found that *en*-negative ac4 or at1 ORNs were not increased concomitantly with the loss of neighboring *en*-positive lineages in *en* mutants (Figure S7A).

In order to simulate combinatorial rules giving rise to the diverse population of SOP identities, we generated a toy Waddington model describing the diversification landscape of early ORN precursor fates prior to the onset of asymmetric divisions by nesting the regulatory relationships between the transcription factors. This allowed us to create a decision landscape that can be modified by changing the state of each transcription factor in precursors from the matrix of transcription factors listed in the order of their temporal expression in the antennal disc. Therefore, a smooth plane of precursors can be modified into more complex landscapes where the addition of each factor creates a dip from a prior state that defines a new precursor fate (Figure 7B; Supplemental Experimental Procedures). This computational simulation not only allows us to visualize the outcome of the ORN precursor diversification process as a whole but also leads to predictions about the decision landscapes for different mutant conditions (single- or double-mutant combinations) through modifying input parameters in the transcription factor matrix (Figures 5 and 7B; Figure S5). The model successfully reproduces ORN diversity landscapes of some experimentally testable single and double mutants (Figures 5 and 7; Figure S7B). Systems-level dynamic analysis of olfactory receptor gene regulation during development in the future will enable us to more thoroughly explore the decision cascade of ORNs from a diverse array of precursors to refine this model.

Discussion

Neuronal diversity is a common characteristic of all sensory systems throughout the animal kingdom. Among these, the olfactory system demonstrates an extreme case in its diversity of ORN classes. In *Drosophila*, each of the 50 adult ORN classes is defined by the unique expression of typically a single olfactory receptor from a pool of around 80 genes [2, 4, 5]. How this ORN diversity is generated from a field of homogeneous precursor cells during development remains elusive. Combinatorial control of transcription factors has been proposed as an important mechanism that complex systems utilize to create cellular diversity [24–26]. Here, we demonstrate the nested and binary combinatorial rules by which transcription factors interact with each other to guide decisions regarding ORN precursor identities. Our results suggest that nesting the regulatory relationship of transcription factor combinations allows the concurrent use of the same factors in parallel lineages to generate ORN diversity in a very efficient manner. Under this logic, binary lineage choices in precursor cells are made based on historical contingency, which could serve as an effective strategy for establishing cellular complexity in many other developing systems.

In both vertebrates and invertebrates, each ORN class is spatially restricted to specific zones within the peripheral olfactory organs. In *Drosophila*, antennal ORNs are housed in three morphologically and topographically different types of sensilla occupying distinct zones, while maxillary palps have only a single type of sensilla [2]. Each of the sensilla type zones on the antenna are subdivided into subzones that are defined by sensilla subtypes, which have similar morphology but differ in the set of olfactory receptors expressed in the ORNs they house [2]. It has been shown that the decision for a given palp-specific olfactory receptor gene to be expressed in maxillary palp ORNs, but not in antennal ORNs, requires both positive and negative regulatory elements around that gene [27, 28]. For antennal ORNs, the proneural genes *amos* and *ato* and the prepatterning gene *lz* were found to assign sensilla type identities to the precursors and determine olfactory receptors expressed by the neurons housed in these sensilla (Figure 7) [6–8]. The loss of Amos or Ato leads to the complete loss of basiconic and trichoid or coeloconic sensilla types, respectively, and corresponding ORNs. Lz diversifies sensilla type identities within the Amos-expressing lineage, where high levels of Lz are associated with basiconic sensilla fates, versus low levels of Lz, which generates ORNs in trichoid sensilla [9, 15]. Hypomorphic alleles of *lz* result in basiconic-totrichoid sensilla type conversions [9, 15]. Lz is also required for the expression of Amos, suggesting the existence of regulatory loops among transcription factors in the same network [8]. Our results explain how the next level of diversification occurs following sensilla type specification in the antenna. Rn is expressed in a subset of antennal sensilla precursors and splits precursors of each zone into *rn*-positive and *rn*-negative subtypes. In *rn* mutants, ORN diversity decreases almost by half as ORN classes from *rn*-positive subtypes are switched to *rn*-negative identities within the same zone. Our results suggest that Rn is required to branch off novel precursor identities from default ones, resulting in the generation of new ORN classes in a zone-specific manner. It should be noted that some *rn*-negative sensilla subtypes, for example at2 and ac3, neither decrease nor increase in their numbers in *rn* mutants, suggesting that there are additional factors driving the diversification of the ORN classes in these sensilla. Similarly, further diversification of *rn*-positive ORN precursors should also be under the control of additional factors, such as En, operating in concert with Rn function.

Our results along with others suggest a two-step mechanism for ORN diversification: (1) successive restrictions on precursor differentiation potentials by spatiotemporal factors, such as proneural/prepatterning gene products and Rn, and (2) segregation of restricted fates through Notch-mediated asymmetric divisions and local transcription factor networks for directly turning on olfactory receptor expression. Hypothetically, the sensilla precursor differentiation potentials can be represented by distinct sets of olfactory receptor genes being organized into euchromatic regions in a lineage-specific manner. The aforementioned combinations of transcription factors may influence the dynamics of such epigenetic states, resulting in limited combinations of receptors transcriptionally accessible for later stages of ORN differentiation. Examples of chromatin modulation in OR expression have been demonstrated in both flies and mice [29–31]. Once precursor potentials are set, the Notch signaling pathway could continue to bifurcate alternate sensory identities into ORNs generated through asymmetric precursor cell divisions [13, 32]. Transcription factor networks expressed later in development, including the well-characterized Acj6, Pdm3, and

Scalloped, could then directly regulate olfactory receptor expression during these divisions based on their genomic accessibility, giving rise to terminally differentiated ORNs [27, 28, 33–35].

In comparison with the *Drosophila* olfactory system, mammals exhibit remarkable organizational similarities in the olfactory circuitry, even though the numerical complexity far exceeds that of their insect counterparts. For example, the zonal pattern of olfactory receptor expression in the mammalian olfactory epithelium is analogous to the topographic segregation of sensilla type-dependent olfactory receptor expression in the antenna [36]. A number of transcription factors were reported to regulate the zone-specific expression of a subset of olfactory receptors, yet no mutants resulting in ORN sensory conversion have been described [37–39]. Despite the consensus on the stochastic nature of mammalian olfactory receptor expression within each zone, it would be interesting to see whether the zones are defined by a similar developmental strategy.

The model we present here also provides us with an ancestral precursor decision landscape that reveals the interaction pattern among factors to maintain and modify phenotypic complexity and diversity within sensory neural circuits on evolutionary timescales. New regulatory nodes might be added to the combinatorial code at distinct stages of precursor cell development to change ORN specification programs. For example, addition of *mir-279*, a negative regulator of the transcription factor *nerfin-1* expressed in maxillary palp ORN precursors, results in the elimination of CO_2-sensory ORNs from specific maxillary palp sensilla [14]. Furthermore, olfactory receptor genes have been shown to be fast evolving across and within genomes [40, 41]. Incremental addition of individual regulatory modules to preexisting lineage-specific combinations operating in binary ON/OFF mode could facilitate the coordination of novel ORN fates with the evolution of receptor genes, which can be modified in response to changes in the quantity, quality, and context of the olfactory environment.

Supplementary Material

Refer to Web version on PubMed Central for supplementary material.

Acknowledgments

We are grateful to Hugo Bellen, Andrew Jarman, and Richard Benton for providing fly stocks and antibodies. We thank the Duke Light Microscopy Core Facility and Model System Genomics for great technical assistance; Uwe Ohler, Amy Schmid, and Katia Koelle for discussions on modeling; and Hiro Matsunami, Dave McClay, Amy Bejsovec, Paul Durst, and members of the Volkan laboratory for discussions and comments on the manuscript. P.C.V. is supported by the Whitehall Foundation. This project is funded by NIH grant R01DC02539 to D.P.S. and Duke University startup funds to P.C.V.

References

1. Rodrigues V, Hummel T. Development of the Drosophila olfactory system. Adv. Exp. Med. Biol. 2008; 628:82–101. [PubMed: 18683640]
2. Couto A, Alenius M, Dickson BJ. Molecular, anatomical, and functional organization of the Drosophila olfactory system. Curr. Biol. 2005; 15:1535–1547. [PubMed: 16139208]

3. Clyne PJ, Warr CG, Freeman MR, Lessing D, Kim J, Carlson JR. A novel family of divergent seven-transmembrane proteins: candidate odorant receptors in Drosophila. Neuron. 1999; 22:327–338. [PubMed: 10069338]

4. Benton R, Vannice KS, Gomez-Diaz C, Vosshall LB. Variant ionotropic glutamate receptors as chemosensory receptors in Drosophila. Cell. 2009; 136:149–162. [PubMed: 19135896]

5. Fishilevich E, Vosshall LB. Genetic and functional subdivision of the Drosophila antennal lobe. Curr. Biol. 2005; 15:1548–1553. [PubMed: 16139209]

6. Gupta BP, Rodrigues V. Atonal is a proneural gene for a subset of olfactory sense organs in Drosophila. Genes Cells. 1997; 2:225–233. [PubMed: 9189759]

7. zur Lage PI, Prentice DR, Holohan EE, Jarman AP. The Drosophila proneural gene amos promotes olfactory sensillum formation and suppresses bristle formation. Development. 2003; 130:4683–4693. [PubMed: 12925594]

8. Goulding SE, zur Lage P, Jarman AP. amos, a proneural gene for Drosophila olfactory sense organs that is regulated by lozenge. Neuron. 2000; 25:69–78. [PubMed: 10707973]

9. Gupta BP, Flores GV, Banerjee U, Rodrigues V. Patterning an epidermal field: Drosophila lozenge, a member of the AML-1/Runt family of transcription factors, specifies olfactory sense organ type in a dose-dependent manner. Dev. Biol. 1998; 203:400–411. [PubMed: 9808789]

10. Ha TS, Smith DP. A pheromone receptor mediates 11-cis-vaccenyl acetate-induced responses in Drosophila. J. Neurosci. 2006; 26:8727–8733. [PubMed: 16928861]

11. St Pierre SE, Galindo MI, Couso JP, Thor S. Control of Drosophila imaginal disc development by rotund and roughened eye: differentially expressed transcripts of the same gene encoding functionally distinct zinc finger proteins. Development. 2002; 129:1273–1281. [PubMed: 11874922]

12. Silbering AF, Rytz R, Grosjean Y, Abuin L, Ramdya P, Jefferis GS, Benton R. Complementary function and integrated wiring of the evolutionarily distinct Drosophila olfactory subsystems. J. Neurosci. 2011; 31:13357–13375. [PubMed: 21940430]

13. Endo K, Aoki T, Yoda Y, Kimura K, Hama C. Notch signal organizes the Drosophila olfactory circuitry by diversifying the sensory neuronal lineages. Nat. Neurosci. 2007; 10:153–160. [PubMed: 17220884]

14. Cayirlioglu P, Kadow IG, Zhan X, Okamura K, Suh GS, Gunning D, Lai EC, Zipursky SL. Hybrid neurons in a microRNA mutant are putative evolutionary intermediates in insect CO2 sensory systems. Science. 2008; 319:1256–1260. [PubMed: 18309086]

15. Bhalerao S, Sen A, Stocker R, Rodrigues V. Olfactory neurons expressing identified receptor genes project to subsets of glomeruli within the antennal lobe of Drosophila melanogaster. J. Neurobiol. 2003; 54:577–592. [PubMed: 12555270]

16. Bailey TL, Williams N, Misleh C, Li WW. .MEME: discovering and analyzing DNA and protein sequence motifs. Nucleic Acids Res. 2006; 34(Web Server issue):W369–W373. [PubMed: 16845028]

17. Narlikar L, Gordân R, Ohler U, Hartemink AJ. Informative priors based on transcription factor structural class improve de novo motif discovery. Bioinformatics. 2006; 22:e384–e392. [PubMed: 16873497]

18. Pavesi G, Mereghetti P, Mauri G, Pesole G. Weeder Web: discovery of transcription factor binding sites in a set of sequences from co-regulated genes. Nucleic Acids Res. 2004; 32(Web Server issue):W199–W203. [PubMed: 15215380]

19. Bailey TL, Gribskov M. Combining evidence using p-values: application to sequence homology searches. Bioinformatics. 1998; 14:48–54. [PubMed: 9520501]

20. Deplancke B, Vermeirssen V, Arda HE, Martinez NJ, Walhout AJ. Gateway-compatible yeast one-hybrid screens. CSH Protoc. 2006; 2006 http://dx.doi.org/10.1101/pdb.prot4590.

21. Pruneda-Paz JL, Breton G, Para A, Kay SA. A functional genomics approach reveals CHE as a component of the Arabidopsis circadian clock. Science. 2009; 323:1481–1485. [PubMed: 19286557]

22. Baanannou A, Mojica-Vazquez LH, Darras G, Couderc JL, Cribbs DL, Boube M, Bourbon HM. Drosophila distal-less and Rotund bind a single enhancer ensuring reliable and robust bric-abrac2

expression in distinct limb morphogenetic fields. PLoS Genet. 2013; 9:e1003581. [PubMed: 23825964]

23. Song E, de Bivort B, Dan C, Kunes S. Determinants of the Drosophila odorant receptor pattern. Dev. Cell. 2012; 22:363–376. [PubMed: 22340498]
24. Puri PL, Mercola M. BAF60 A, B, and Cs of muscle determination and renewal. Genes Dev. 2012; 26:2673–2683. [PubMed: 23222103]
25. Chlon TM, Crispino JD. Combinatorial regulation of tissue specification by GATA and FOG factors. Development. 2012; 139:3905–3916. [PubMed: 23048181]
26. Baumgardt M, Miguel-Aliaga I, Karlsson D, Ekman H, Thor S. Specification of neuronal identities by feedforward combinatorial coding. PLoS Biol. 2007; 5:e37. [PubMed: 17298176]
27. Ray A, van der Goes van Naters W, Carlson JR. A regulatory code for neuron-specific odor receptor expression. PLoS Biol. 2008; 6:e125. [PubMed: 18846726]
28. Bai L, Carlson JR. Distinct functions of acj6 splice forms in odor receptor gene choice. J. Neurosci. 2010; 30:5028–5036. [PubMed: 20371823]
29. Magklara A, Yen A, Colquitt BM, Clowney EJ, Allen W, Markenscoff-Papadimitriou E, Evans ZA, Kheradpour P, Mountoufaris G, Carey C, et al. An epigenetic signature for monoallelic olfactory receptor expression. Cell. 2011; 145:555–570. [PubMed: 21529909]
30. Sim CK, Perry S, Tharadra SK, Lipsick JS, Ray A. Epigenetic regulation of olfactory receptor gene expression by the Myb-MuvB/dREAM complex. Genes Dev. 2012; 26:2483–2498. [PubMed: 23105004]
31. Clowney EJ, LeGros MA, Mosley CP, Clowney FG, Markenskoff-Papadimitriou EC, Myllys M, Barnea G, Larabell CA, Lomvardas S. Nuclear aggregation of olfactory receptor genes governs their monogenic expression. Cell. 2012; 151:724–737. [PubMed: 23141535]
32. Endo K, Karim MR, Taniguchi H, Krejci A, Kinameri E, Siebert M, Ito K, Bray SJ, Moore AW. Chromatin modification of Notch targets in olfactory receptor neuron diversification. Nat. Neurosci. 2012; 15:224–233. [PubMed: 22197833]
33. Tichy AL, Ray A, Carlson JR. A new Drosophila POU gene, pdm3, acts in odor receptor expression and axon targeting of olfactory neurons. J. Neurosci. 2008; 28:7121–7129. [PubMed: 18614681]
34. Clyne PJ, Certel SJ, de Bruyne M, Zaslavsky L, Johnson WA, Carlson JR. The odor specificities of a subset of olfactory receptor neurons are governed by Acj6, a POU-domain transcription factor. Neuron. 1999; 22:339–347. [PubMed: 10069339]
35. Jafari S, Alkhori L, Schleiffer A, Brochtrup A, Hummel T, Alenius M. Combinatorial activation and repression by seven transcription factors specify Drosophila odorant receptor expression. PLoS Biol. 2012; 10:e1001280. [PubMed: 22427741]
36. Fuss SH, Ray A. Mechanisms of odorant receptor gene choice in Drosophila and vertebrates. Mol. Cell. Neurosci. 2009; 41:101–112. [PubMed: 19303443]
37. Hirota J, Omura M, Mombaerts P. Differential impact of Lhx2 deficiency on expression of class I and class II odorant receptor genes in mouse. Mol. Cell. Neurosci. 2007; 34:679–688. [PubMed: 17350283]
38. Kolterud A, Alenius M, Carlsson L, Bohm S. The Lim homeobox gene Lhx2 is required for olfactory sensory neuron identity. Development. 2004; 131:5319–5326. [PubMed: 15456728]
39. McIntyre JC, Bose SC, Stromberg AJ, McClintock TS. Emx2 stimulates odorant receptor gene expression. Chem. Senses. 2008; 33:825–837. [PubMed: 18854508]
40. Sánchez-Gracia A, Vieira FG, Rozas J. Molecular evolution of the major chemosensory gene families in insects. Heredity (Edinb.). 2009; 103:208–216. [PubMed: 19436326]
41. Kambere MB, Lane RP. Co-regulation of a large and rapidly evolving repertoire of odorant receptor genes. BMC Neurosci. 2007; 8(Suppl 3):S2. [PubMed: 17903278]

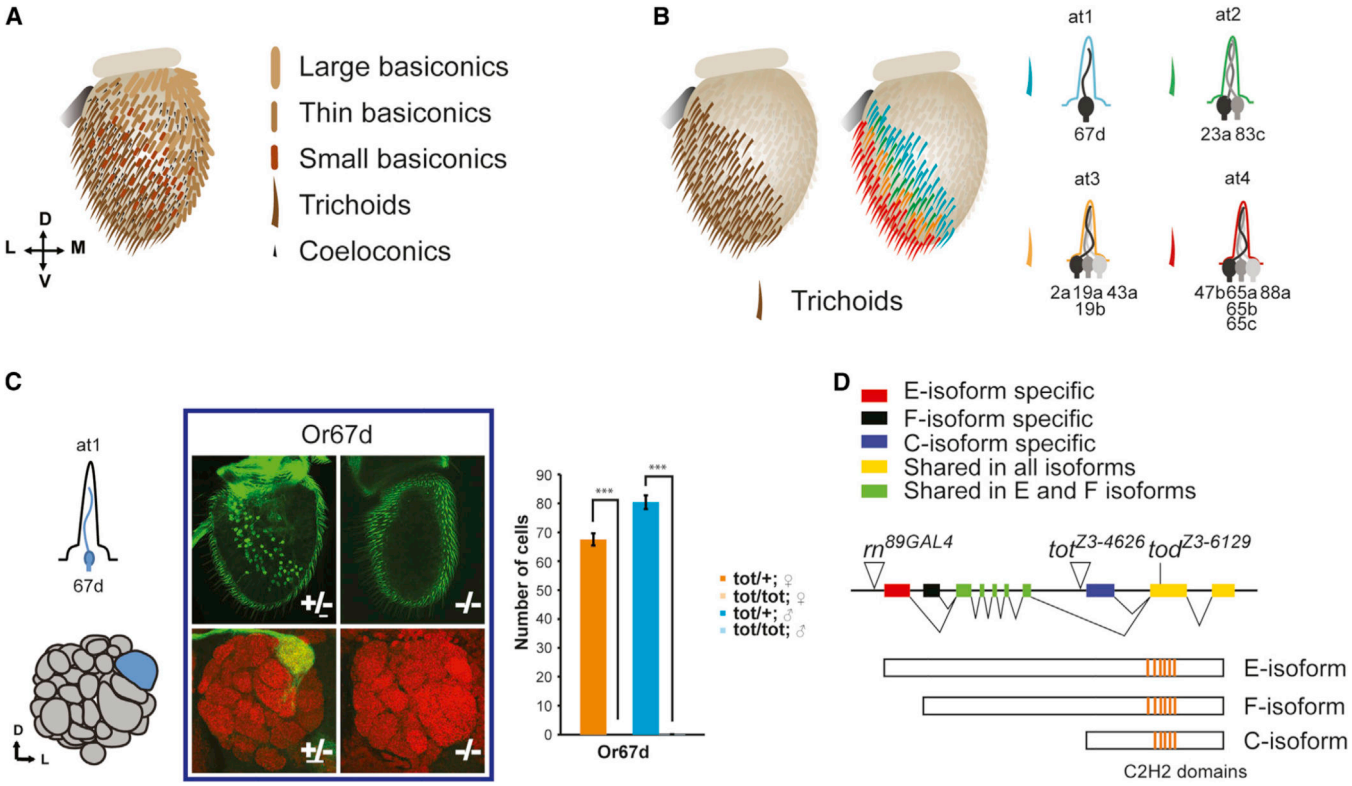

Figure 1. Anatomical Organization of Antennal Sensilla and Molecular Characterization of *rn* Mutants

(A) Spatial organization of sensilla types on the antenna. Trichoid, basiconic (large, thin, and small), and coeloconic sensilla occupy distinct zones. Rare intermediate sensilla are not shown.

(B) Subsegmentation of the trichoid sensilla type into subtypes (at1–at4) is exemplified on the right. ORNs in each subtype express an invariable combination of OR genes (Or19a and Or19b are coexpressed; Or65a, Or65b, and Or65c are coexpressed).

(C) Loss of Or67d-expressing ORNs in *rn* mutants. z projections of confocal stacks for antennae and antennal lobes are shown in the top and bottom panels, respectively. Anti-Bruchpilot staining lights up the antennal lobe neuropil (red). *Or67d*^{GAL4}-mediated CD8 GFP expression is in green. Graph shows quantification of cell body counts. n = 10–15, ***$p < 0.001$. Error bars indicate SEM.

(D) *rn* genomic locus describing different splice isoforms and mutant alleles used in our studies.

See also Figure S1.

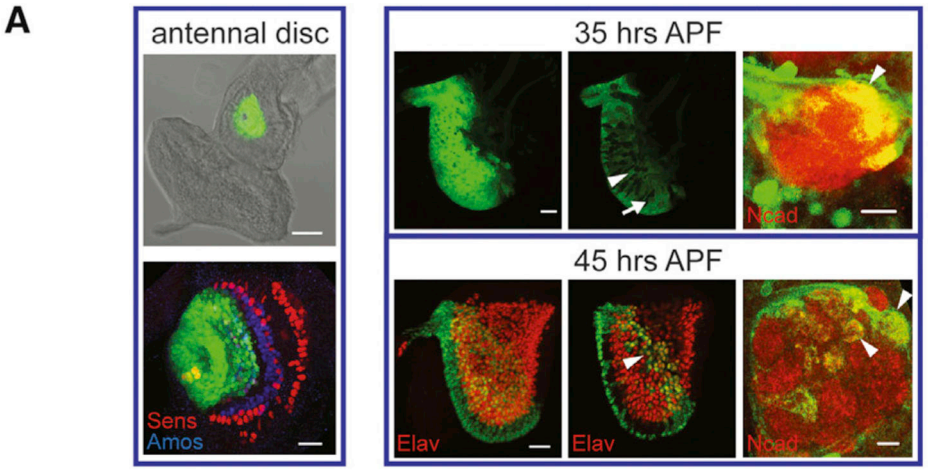

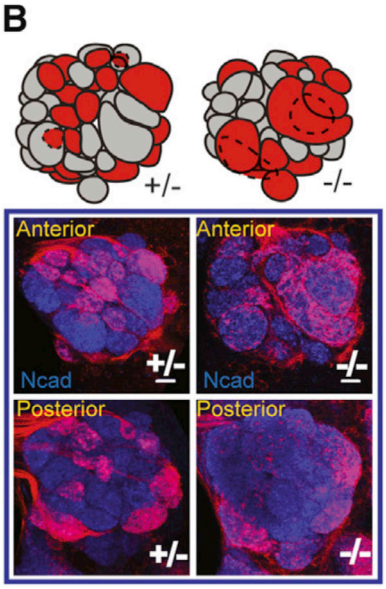

Summary of Rn-positive ORNs in lineage-tracing experiment

	Sensilla type	Subtype	Rotund reporter positive ORNs
WT	trichoid	at1	Or67d
		at3	Or2a, Or19a/b, Or43a
	basiconic	ab5 (thin)	Or82a, Or47a/33b
		ab7 (small)	Or98a, Or67c
		ab10 (small)	Or49a/Or85f, Or67a
	coeloconic	ac1	IR31a, IR75d, IR92a/IR76b
		ac4	IR84a, IR75d, IR76a/IR76b
	intermediate	ai1	Or13a, ? (VA7m)
rn	trichoid	at4	Or47b, Or88a, Or65a/b/c
	basiconic	ab1* (large)	Gr21a, Or92a, Or10a/Gr10a, Or42b
		ab9* (small)	Or67b, Or69aA/B
	coeloconic	ac2	IR75a, IR75d, IR41a/IR76b

*Only seen in female mutants.

Figure 2. Rotund Is Expressed in Subsets of Antennal SOPs

(A) *rn* expression in the developing olfactory system revealed by rn^{89GAL4}-driven UAS-CD8 GFP (green). Senseless (red) and Amos (blue) antibody staining on a 0 hr after puparium formation (APF) antennal disc are shown. Arrowheads point to *rn*-positive ORN cell bodies in the 35 and 45 hr APF antennal images, and their targeting in the pupal antennal lobe. Arrows indicate *rn*-negative cell bodies. Elav (red) labels neurons. N-cadherin (red) antibody labels the pupal antennal lobe neuropil. The middle panels in 35 and 45 hr APF are single confocal sections; all others are z projections. Scale bars in all images are 10 μm except for the bright-field antennal disc image, which is 50 μm.

(B) Lineage tracing using a tub-FRT-nYFP-FRT-CD2 RFP Flp-out cassette driven by rn^{89GAL4} UAS-FLP labels *rn*-positive ORNs (red) in wild-type (left) and *rn* mutant (right) adult antennal lobes. Only anterior and posterior confocal slices from female brains are shown. N-cadherin is in blue. Red glomeruli in the antennal lobe schemes represent target sites for *rn*-positive ORNs. Posterior glomeruli are outlined with dotted lines. The table

shows the list of *rn*-positive ORNs and corresponding sensilla types/subtypes in wild-type (top) and *rn* mutants (bottom). Question marks indicate unmapped *rn*-positive glomeruli. See also Figure S2.

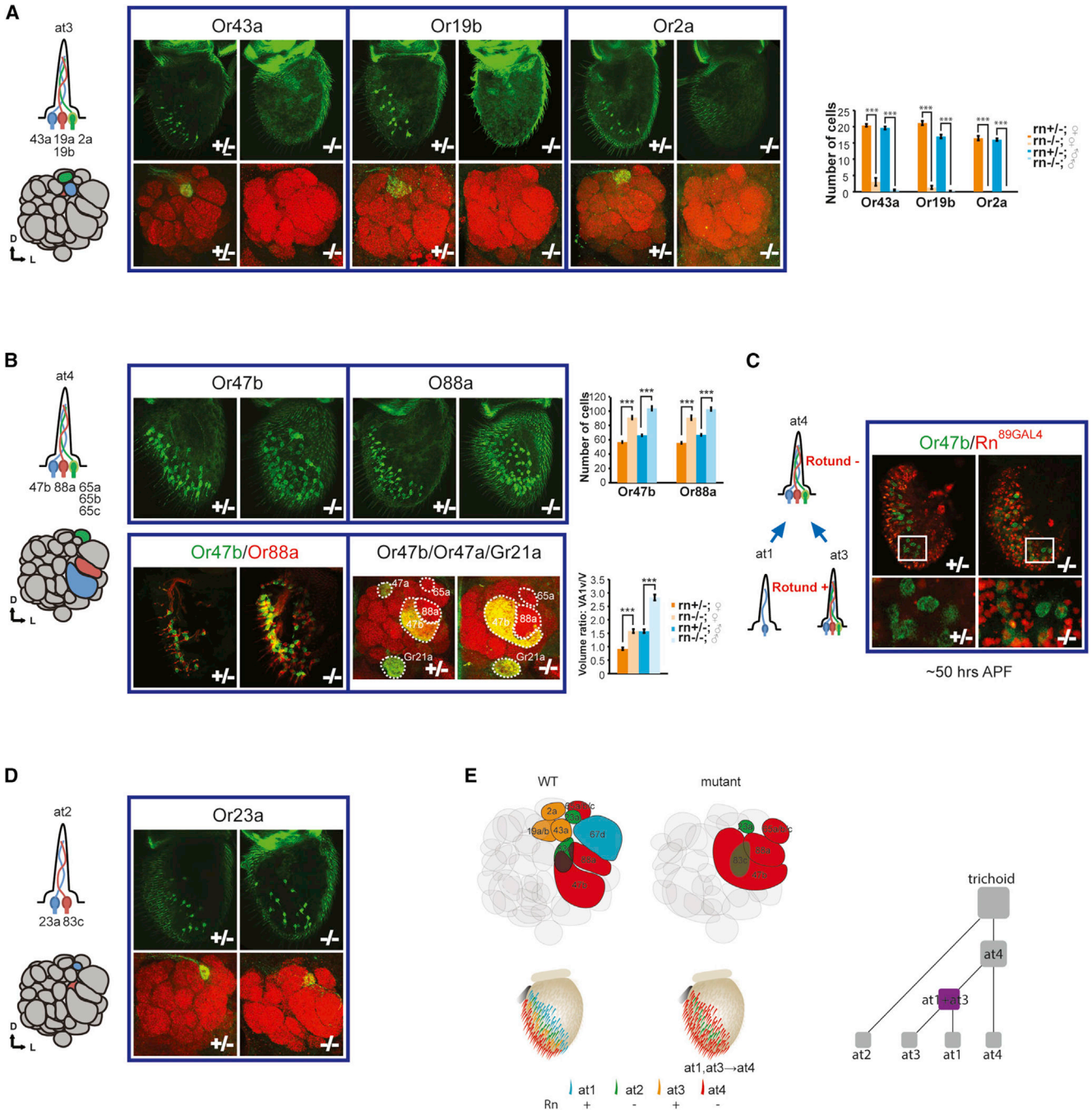

Figure 3. Diversification of New Trichoid Precursor/ORN Identities from Default *rn*-Negative Ones by Rn

(A) Loss of OR expression in at3 sensilla in *rn* mutants. Data are presented similarly as in Figure 1C.

(B) at4 OR expression is expanded to new antennal territories in *rn* mutants (top). Double labeling of Or88a and Or47b ORNs (bottom left) shows correct at4 OR pairings in expanded zones. Or47b, Or88a, and Or65a glomerular volumes are increased in *rn* mutants. Quantification of Or47b volume is shown with Gr21a V glomerulus as the reference (bottom

right). Or47b, Or47a, and Gr21a glomeruli were labeled by synaptotagmin GFP transgenes on the same chromosome [14]. Selected glomeruli were outlined. Note that the Or47a glomerulus is absent in the mutant (see below). n = 10–12. ***p < 0.001. Error bars represent SEM.

(C) *rn*^{89GAL4} UAS-Redstinger (red) expression is normally excluded from Or47b ORNs (green) in at4 sensilla. In *rn* mutants, an additional population of Or47b ORNs that is labeled by *rn* reporter is apparent, indicating sensory conversion from at1 and at3 to at4. Single confocal sections are shown. Bottom panels show higher magnification.

(D) Or23a expression in *rn*-negative at2 trichoid sensilla ORNs is unaffected in *rn* mutants.

(E) Schematic summary depicting conversion of at1 and at3 ORNs to an at4 sensilla identity is shown on the left, and lineage decision tree for trichoid sensilla subtype precursor diversification on the right. The purple square designates *rn*-positive precursor identities diverged from the default *rn*-negative at4.

See also Figures S1, S3A, and S3G.

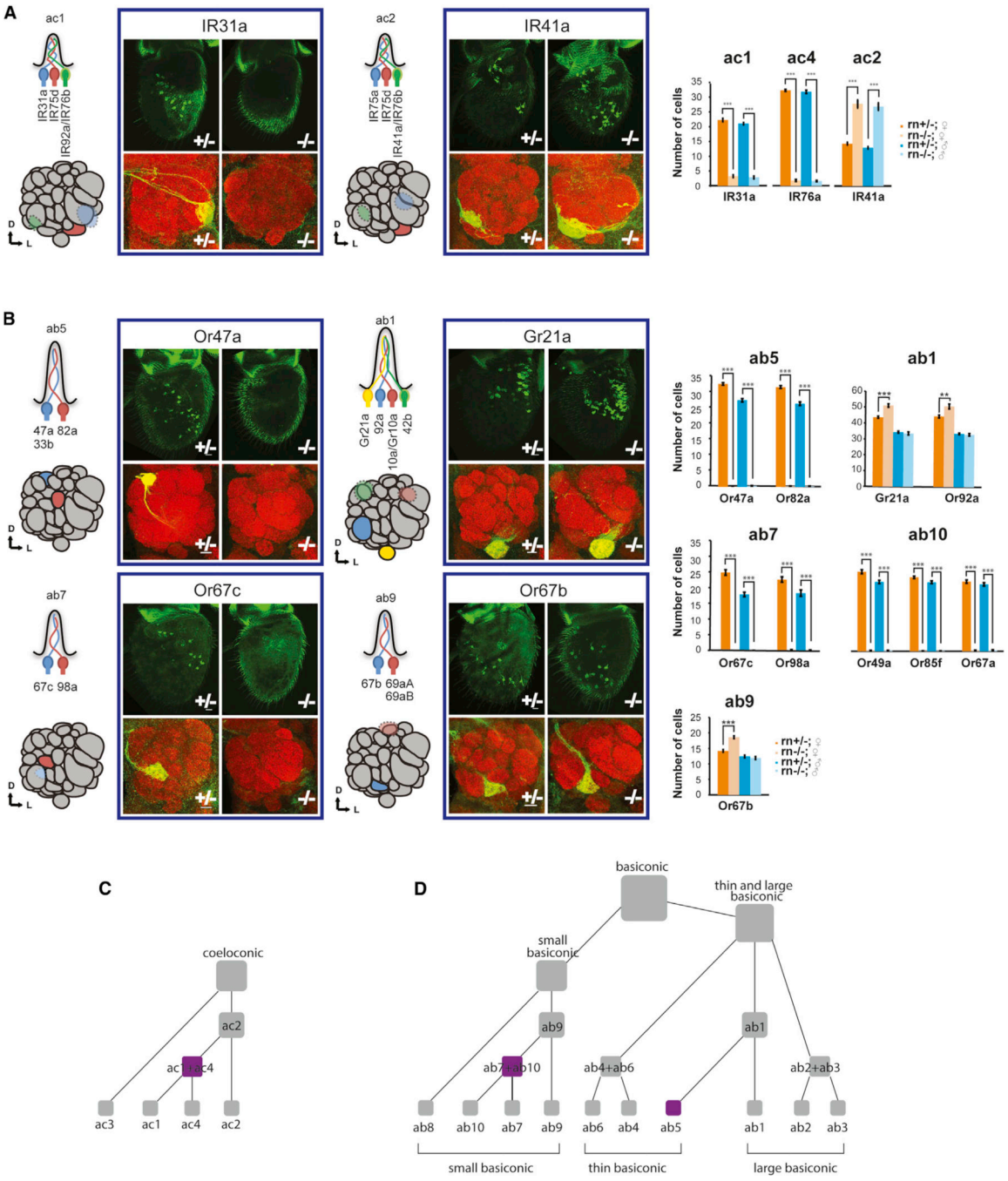

Figure 4. Diversification of New Precursor/ORN Identities from Default *rn*-Negative Ones in Coeloconic and Basiconic Lineages by Rn

(A) Loss of IR expression in *rn*-positive coeloconic ORNs in mutants (left). An ectopic population of *rn*-negative ac2 ORNs expands to new antennal territories. IR41a glomerulus appears larger in *rn* mutants (right).

(B) Loss of OR expression in *rn*-positive basiconic ORNs in mutants (left). *rn*-negative ORNs from ab1 and ab9 sensilla show a slight increase in female mutants (right; images were from female flies). In (A) and (B), data are presented similarly as in Figure 1C.

(C and D) Lineage decision trees for coeloconic and basiconic sensilla subtype precursor diversification, respectively. The purple squares designate *rn*-positive precursor identities diverged from the default *rn*-negative ones. For basiconics, we believe that *rn*-positive ab5 (thin basiconic) diverged from the default *rn*-negative ab1 (large basiconic) identity across morphological subdivisions. At this point, developmental markers to confirm this diversification pattern are unavailable.
See also Figures S3 and S4.

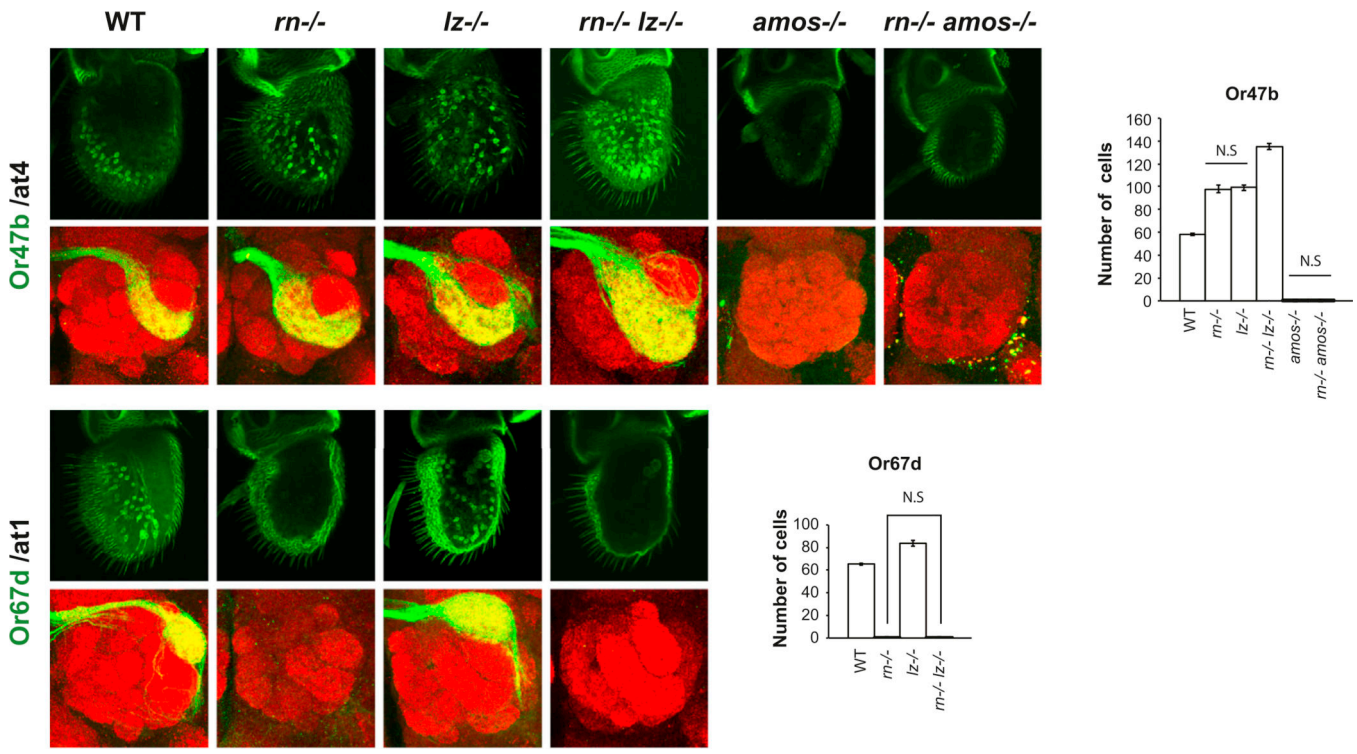

Figure 5. Effects of *rn*, *lz*, and *amos* Single Mutants and *rn/lz* and *rn/amos* Double Mutants on ORN Specification

rn and *lz* incrementally affect the number of Or47b neurons in at4 sensilla that are dependent on *amos*. *lz* functions similarly in at1 and at4, as both Or67d and Or47d neurons expand to new antennal zones in *lz* single mutants. The specification of Or67d neurons also requires *rn*. For antennal lobes, Or47b glomerular sizes are $rn^{-/-}$ $lz^{-/-}$ > $rn^{-/-}$ or $lz^{-/-}$ > WT. Or67d glomerulus in $lz^{-/-}$ is bigger than that in WT. In $amos^{-/-}$ and $rn^{-/-}$ $amos^{-/-}$, many glomeruli in the anterior region of antennal lobe are missing, including Or47b. In $rn^{-/-}$ and $rn^{-/-}$ $lz^{-/-}$, Or67d glomerulus is missing. Graph shows the quantification of cell body counts. n = 10–15. Differences between samples from different genotypes are all statistically significant except for the labeled pairs. $p < 0.001$. Error bars indicate SEM.

See also Figure S5.

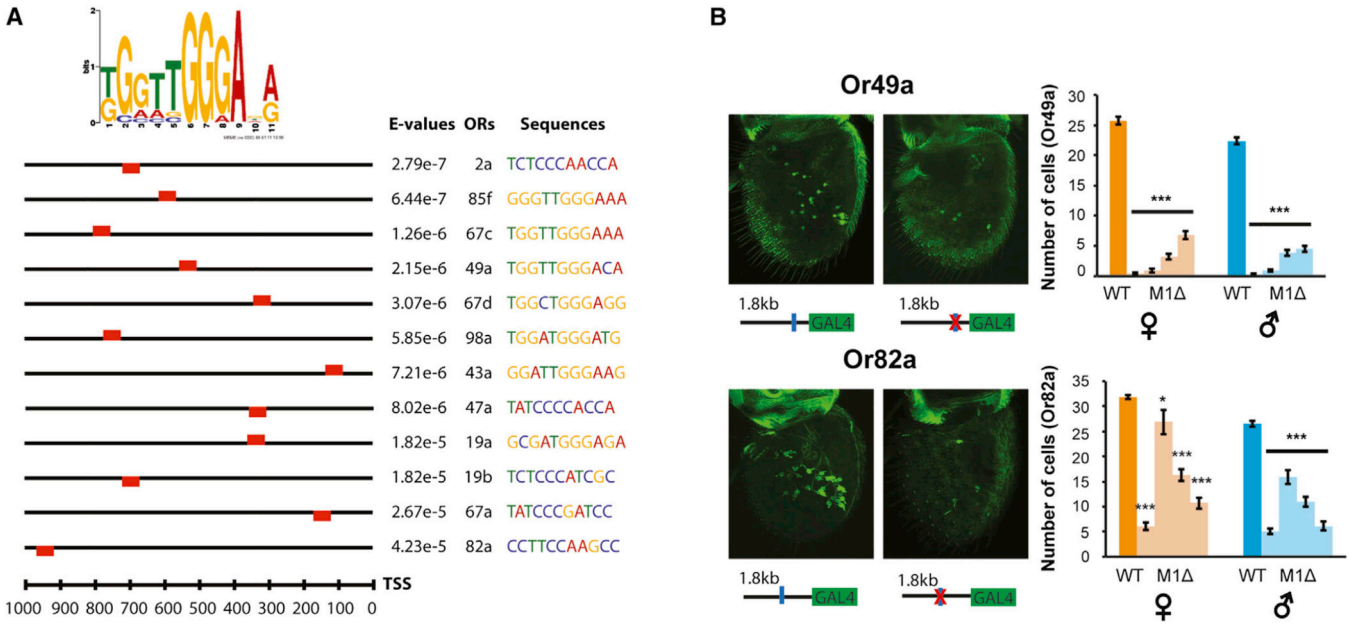

Figure 6. Requirement of the M1 Motif Upstream of *rn*-positive Olfactory Receptor Genes for Appropriate OR Expression

(A) M1 consensus motif upstream of *rn*-positive ORs discovered by de novo motif finding approach (MEME). Axis indicates number of base pairs upstream from TSS of each OR gene, and red boxes indicate locations of motif occurrences. Boxes above line indicate that the original version of motif was found; boxes below line indicate that the reverse complement was found.

(B) Replacement of the M1 motif with a random sequence in *rn*-positive Or49a or Or82a promoter GAL4 reporter transgenes dramatically decreases their antennal expression. Four independent lines (in lighter shades) were randomly chosen for each gender in both Or49a and Or82a promoter GAL4 transgenes. n = 10–15; ***p < 0.001; *p < 0.05. Error bars indicate SEM.

See also Figure S6.

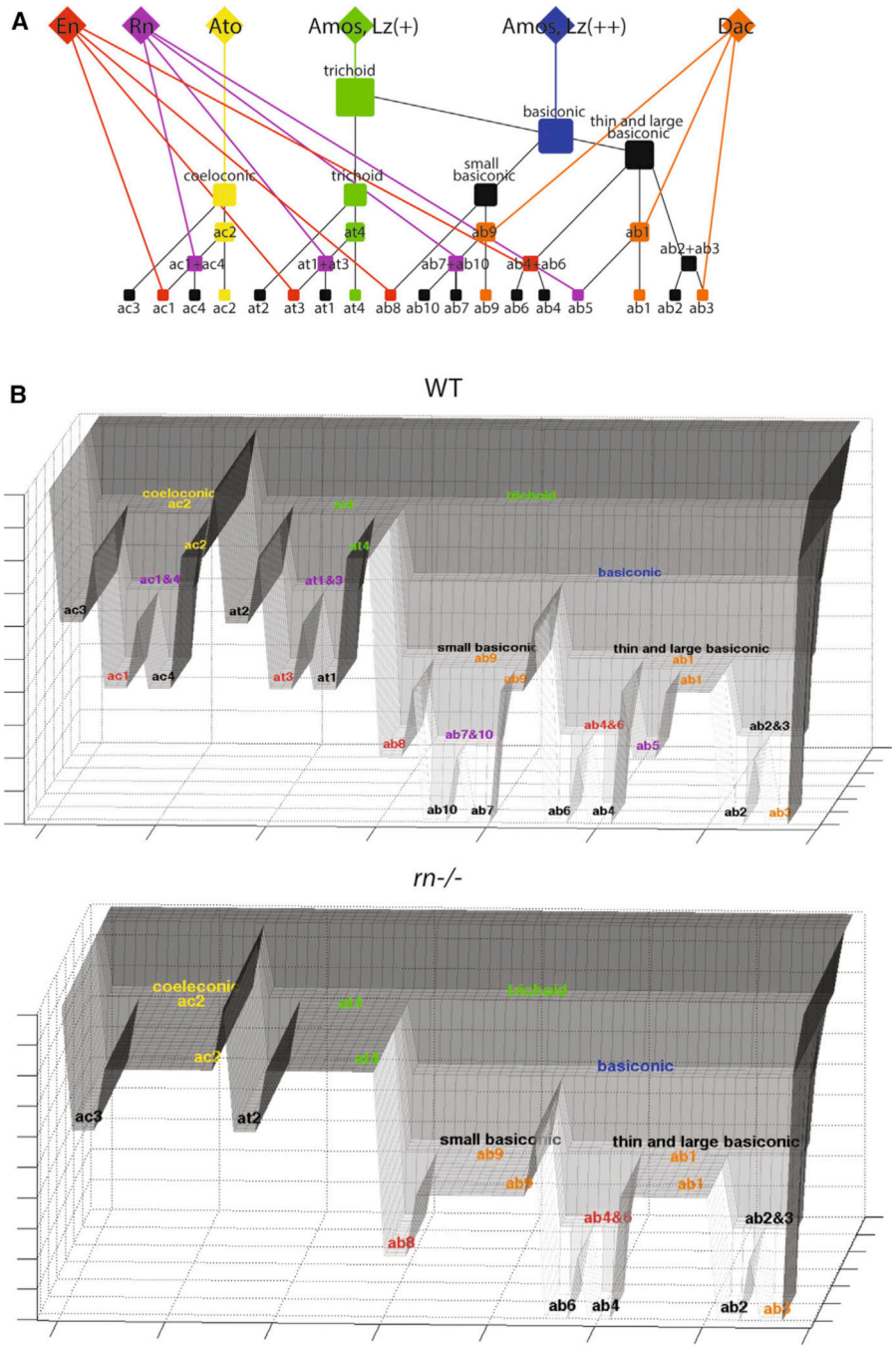

Figure 7. Combinatorial Modulation of ORN Precursor Specification Landscape

(A) Representation of the transcription factors driving ORN precursor diversification. Diamonds represent the following transcription factors: En (Engrailed), Rn (Rotund), Ato (Atonal), Amos, Lz (Lozenge), and Dac (Dachshund). For Lz, "++" indicates a higher level of expression than "+." Squares denote precursor differentiation potentials based on sensilla type/subtype relationships obtained from our results. Sensilla identities determined by lineage-specific transcription factors are shown in color, while the factors differentiating the precursors in black are unaccounted for. Addition of Rn to already existing combinations of

transcription factors in each lineage hierarchically diversifies new precursor identities from default ones.

(B) A toy Waddington model generated in MATLAB (see Supplemental Experimental Procedures) automating the branching relationships in (A) to simulate the diversification of ORN precursor landscape. Simulation for *rn* mutation reshapes the landscape as expected, decreasing the complexity of the landscape (lower image). Each dip/layer designates the emergence of a new precursor identity from existing states generated by the addition of a new factor. The novel ORN pairings depend on what other factors are present in the combinatorial code. Color coding is the same as in (A).

See also Figure S7.